Mineralogical Magazine (2021), **85**, 161–171
doi:10.1180/mgm.2020.100

CAMBRIDGE UNIVERSITY PRESS

Article

Panskyite, $Pd_9Ag_2Pb_2S_4$, a new platinum group mineral from the Southern Kievey ore occurrence of the Fedorova–Pana layered intrusion, Kola Peninsula, Russia

Anna Vymazalová[1*], Viktor V. Subbotin[2], František Laufek[1], Yevgeny E. Savchenko[2], Chris J. Stanley[3], Dmitriy A. Gabov[2] and Jakub Plášil[4]

[1]Czech Geological Survey, Geologická 6, 152 00 Prague, Czech Republic; [2]Geological Institute, Kola Science Centre of the Russian Academy of Sciences, 184209 Apatity, Russia; [3]Department of Earth Sciences, Natural History Museum, London SW7 5BD, UK; and [4]Institute of Physics, AS CR v.v.i. Na Slovance 2, 182 21, Prague 8, Czech Republic

Abstract

Panskyite, $Pd_9Ag_2Pb_2S_4$, is a new mineral (IMA2020–039) discovered in the platinum-group element mineralisation of the Southern Kievey ore occurrence of the Fedorova–Pana layered intrusion, Kola Peninsula, Russia. It forms tiny anhedral grains (of 0.5 to 10 µm in size) in the interstices of rock-forming silicates, often forming tiny inclusions in base-metal sulfides (millerite, chalcopyrite, bornite and chalcocite) and complex intergrowths with other platinum group minerals (zvyagintsevite, laflammeite, vysotskite, thalhammerite, unnamed phase $Pd_9Ag_2(Tl,Pb)_2S_4$ and others). In plane-polarised light, panskyite is creamy white with weak bireflectance, weak pleochroism and distinct anisotropy with brown to grey rotation tints; it exhibits no internal reflections. Reflectance values for panskyite in air (R_1, R_2 in %) are: 43.8, 44.1 at 470 nm; 44.4, 44.7 at 546 nm; 45.6, 45.8 at 589 nm; and 47.2, 47.2 at 650 nm. Twelve electron-microprobe analyses of panskyite gave an average composition: Pd 55.61, Ag 12.36, Pb 23.50, Fe 0.21, Ni 0.24 and S 7.17 total 99.09 wt.%, corresponding to the formula $(Pd_{9.05}Fe_{0.07}Ni_{0.07})_{\Sigma 9.19}Ag_{1.98}Pb_{1.96}S_{3.87}$ based on 17 atoms; the average of nine analyses on the synthetic analogue is: Pd 57.02, Ag 14.17, Pb 21.81 and S 7.44, total 100.44 wt.%, corresponding to $Pd_{9.07}Ag_{2.22}Pb_{1.78}S_{3.93}$. The density, calculated on the basis of the empirical formula, is 9.81 g/cm^3. The mineral is tetragonal, space group *I4/mmm*, with $a = 7.973(3)$, $c = 9.139(3)$ Å, $V = 581.0(4)$ Å^3 and $Z = 2$. The crystal structure was solved from the single-crystal and powder X-ray diffraction data of synthetic $Pd_9Ag_2Pb_2S_4$. Panskyite is isostructural with thalhammerite ($Pd_9Ag_2Bi_2S_4$). The mineral name is for the locality, the Pansky massif of the Fedorova–Pana layered intrusion in the Kola Peninsula, Russia.

Keywords: panskyite, platinum-group mineral, $Pd_9Ag_2Pb_2S_4$, Fedorova–Pana layered intrusion, Kola Peninsula, Russia

(Received 6 November 2020; accepted 5 December 2020; Accepted Manuscript published online: 21 December 2020; Associate Editor: Peter Leverett)

Introduction

Panskyite, $Pd_9Ag_2Pb_2S_4$, is a new platinum-group mineral (PGM) discovered in a sample taken from an outcrop of mineralised anorthosites containing irregular disseminations of sulfides with platinum-group element (PGE) mineralisation in the area of the Southern Kievey ore occurrence Fedorova–Pana layered intrusion, Kola Peninsula, Russia (67°29′04.9″N, 35°35′02″E), Figs 1 and 2. The mineral was also found in low-sulfide ores from the deposits of Kievey and Northern Kamennik of the same intrusion (Fig. 1).

Panskyite is a Pb analogue of thalhammerite ($Pd_9Ag_2Bi_2S_4$). In addition a Tl analogue $Pd_9Ag_2(Tl,Pb)_2S_4$ was observed in samples from Southern Kievey Figs 3 and 4. The Fedorova–Pana layered intrusion is the second known occurrence for thalhammerite and the existence of the Tl analogue is reported for the first time.

A mineral with a similar composition to panskyite was preliminarily described as an unnamed phase Pd_5AgPbS_2 by Subbotin *et al.* (2017). No phase of similar composition is listed among the unnamed minerals of Smith and Nickel (2007).

Both the mineral and its name were approved by the International Mineralogical Association Commission on New Minerals, Nomenclature and Classification (IMA-CNMNC), under the number 2020-039 (Vymazalová *et al.*, 2020). The mineral name is for the locality, the Pansky massif (Cyrillic: Панский массив) of the Fedorova–Pana layered intrusion in the Kola Peninsula, Russia. The name Pansky intrusive massif is the most commonly used term in Russia. It has developed historically and comes from the geographical name of the mountain range – Panskie Tundra Ridge. It is now believed that the Pansky massif unites two independent intrusions: West-Pana and East-Pana (Korchagin and Mitrofanov, 2008). Previously, these two intrusions were considered as tectonic blocks of one intrusion – the Pansky massif (see Fig. 2, Schissel *et al.*, 2002).

*Author for correspondence: Anna Vymazalová, Email: anna.vymazalova@geology.cz
Cite this article: Vymazalová A., Subbotin V.V., Laufek F., Savchenko Y.E., Stanley C.J., Gabov D.A. and Plášil J. (2021) Panskyite, $Pd_9Ag_2Pb_2S_4$, a new platinum group mineral from the Southern Kievey ore occurrence of the Fedorova–Pana layered intrusion, Kola Peninsula, Russia. *Mineralogical Magazine* **85**, 161–171. https://doi.org/10.1180/mgm.2020.100

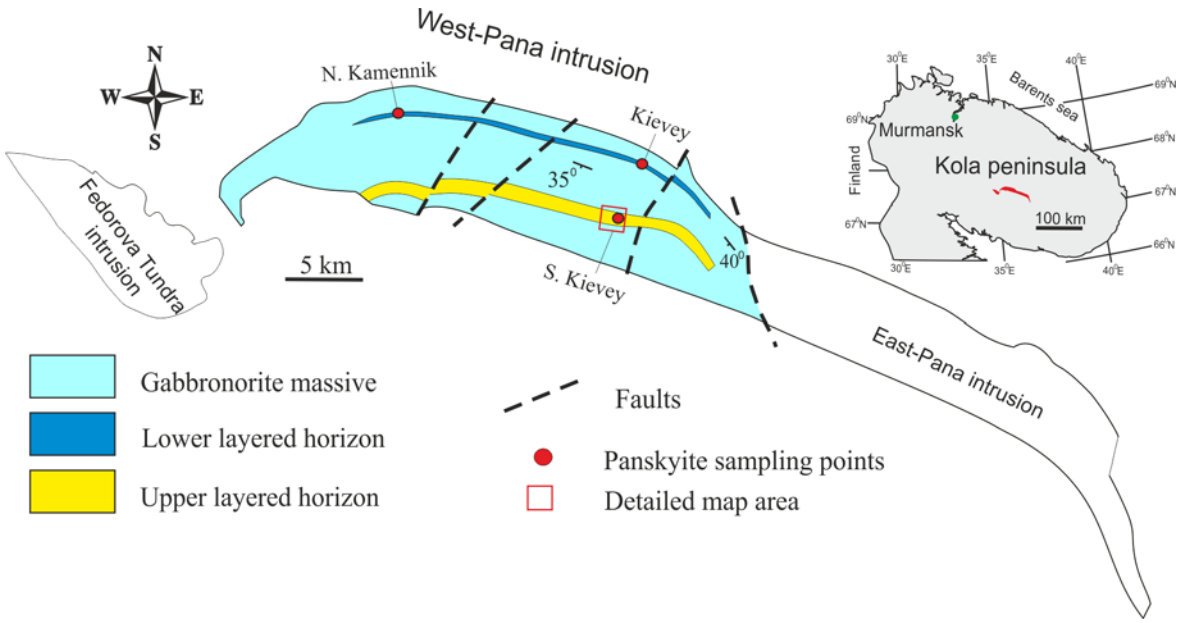

Fig. 1. Schematic geological map of the Fedorova-Pana intrusion (adapted from Subbotin *et al.*, 2019).

Holotype material (polished section), along with its synthetic analogue (experiment number Exp 51), is deposited at the Department of Earth Sciences of the Natural History Museum, London, UK, catalogue number BM 2020,2.

Occurrence

The Fedorova–Pana layered intrusion has a plate-like shape of 80 km long and 0.5 to 6 km wide, with its layering dipping in a south-west direction (Fig. 1). It consists of three separate intrusions: Fedorova Tundra, West-Pana and East-Pana. The Fedorova–Pana complex belongs to a group of Paleoproterozoic layered intrusions distributed in the north-eastern part of the Fenno–Scandian Shield.

The Southern Kievey area, where the holotype specimen was found, is located in the south-eastern part of the West-Pana intrusion in the zone of the Upper Layered Horizon (Fig. 2). It consists of interlayered gabbronorites, norites, leucogabbro and anorthosites and has a thickness of up to 300 m. It contains 0.1–2% disseminated Cu–Ni sulfides and PGE-mineralisation. The main minerals are chalcopyrite, bornite, pentlandite, millerite, vysotskite, braggite, kotulskite, keithconnite, telluropalladinite, sperrylite, stillwaterite, törnroosite and Au–Ag–Pd alloys. Zones containing disseminated sulfides and PGMs form concordant lenses 0.5–2.0 m thick and up to a few hundred metres long near the top and base of the anorthosite bodies. The actual sulfide mineralisation is erratic and discontinuous along strike and dip. This particular level of mineralisation is called the Southern PGE reef (Korchagin and Mitrofanov, 2008).

In other samples, panskyite was found in low-sulfide PGE ores of the Kievey and Northern Kamennik deposits. These deposits are located in the Northern PGE reef in the Lower Layered Horizon zone (Fig. 1). Disseminated sulfides form extended (0.9–6.1 km) layers of variable thickness (0.2–6.5 m) explored to a depth of 250–300 m. The ores contain 0.5–3% base-metal sulfides consisting mainly of chalcopyrite, pentlandite, pyrrhotite and PGM, mainly kotulskite, moncheite, vysotskite, braggite and Au–Ag–Pd alloys. For more information on the geology of these deposits and the mineral composition of the ores, see the publications of Korchagin *et al.* (2009) and Korchagin *et al.* (2016).

In the holotype specimen, panskyite is associated with millerite, pentlandite, violarite, chalcopyrite, bornite, vysotskite, braggite, laflammeite, keithconnite, zvyagintsevite, Au–Ag and Au–Ag–Pd alloys, rock-forming minerals of the plagioclase (labradorite) group, minerals of the amphibole and chlorite groups, clinozoisite and quartz. Other samples (from Southern Kievey, Kievey and Northern Kamennik) contain in addition: magnetite, pyrrhotite, pyrite, siegenite, chalcocite, clausthalite, coldwellite, thalhammerite, laurite, hollingworthite, irarsite, sperrylite, arsenopalladinite, törnroosite, kotulskite, telluropalladinite, telargpalite, lukkulaisvaaraite, Pt–Fe alloy, unnamed phase $Pd_9Ag_2(Tl,Pb)_2S_4$ (the Tl analogue of panskyite) and thalhammerite (Figs 3 and 4).

Panskyite was found in the disseminated low-sulfide PGE-ore. This type of ore was formed in reef zones of the layered intrusions of the Fedorova–Pana complex as a result of processes of liquation and segregation of sulfides during the cooling of the basic melt (Naldrett, 2004; Schissel *et. al.*, 2002). Panskyite was probably formed as a result of relatively low-temperature (<500°C) post-magmatic alterations of low-sulfide PGE ore, in a similar manner to thalhammerite in galena–pyrite–chalcopyrite and millerite–bornite–chalcopyrite vein-disseminated ores from the Komsomolsky mine of the Talnakh and Oktyabrsk deposits, Noril'sk region (Vymazalová *et al.*, 2018).

Appearance and physical and optical properties

In polished sections, panskyite occurs as small individual anhedral grains of 0.5–10 µm in the interstices of rock-forming silicates (Fig. 5). It often intergrows or forms tiny inclusions in base-metal sulfides (millerite, chalcopyrite, bornite and

https://doi.org/10.1180/mgm.2020.100 Published online by Cambridge University Press

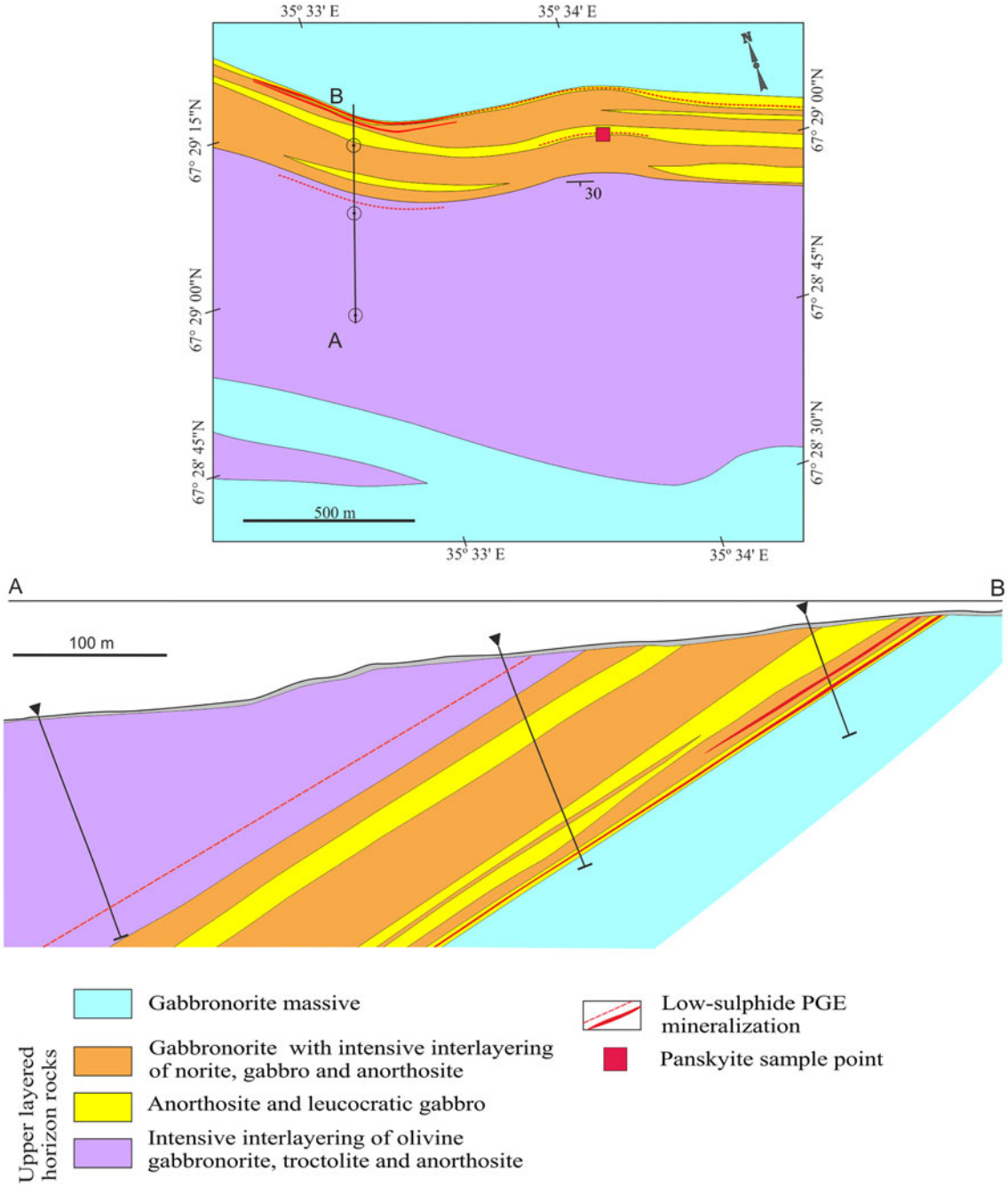

Fig. 2. Geological map and cross-section (A–B) of the Southern Kievey area (adapted from Korchagin and Mitrofanov, 2008).

chalcocite) and forms complex intergrowths with other PGM (zvyagintsevite, laflammeite and vysotskite). Reflected light and back-scattered electron images of panskyite and associated minerals are shown in Fig. 5. Panskyite in intergrowths with its Tl-rich Pb analogue thalhammerite is shown in Fig. 3a,b.

Due to the small grain size and intergrowths with other ore minerals, the physical properties of panskyite could not be determined on natural or synthetic material. Panskyite is opaque and has a metallic lustre. The powder of the synthetic analogue is grey in colour and has a grey streak. The mineral is brittle. The density calculated on the basis of the empirical formula and cell dimensions of panskyite is 9.81 g.cm^{-3}.

In plane-polarised light, panskyite is creamy white. It is weakly bireflectant, weakly pleochroic and it has a distinct anisotropism with brown to grey rotation tints. Internal reflections were not observed.

The reflectance measurements were made in air relative to a WTiC standard on both panskyite and its synthetic analogue using a J & M TIDAS diode array spectrometer attached to a Zeiss Axiotron microscope. The results are given in Table 1 and illustrated in Fig. 6.

https://doi.org/10.1180/mgm.2020.100 Published online by Cambridge University Press

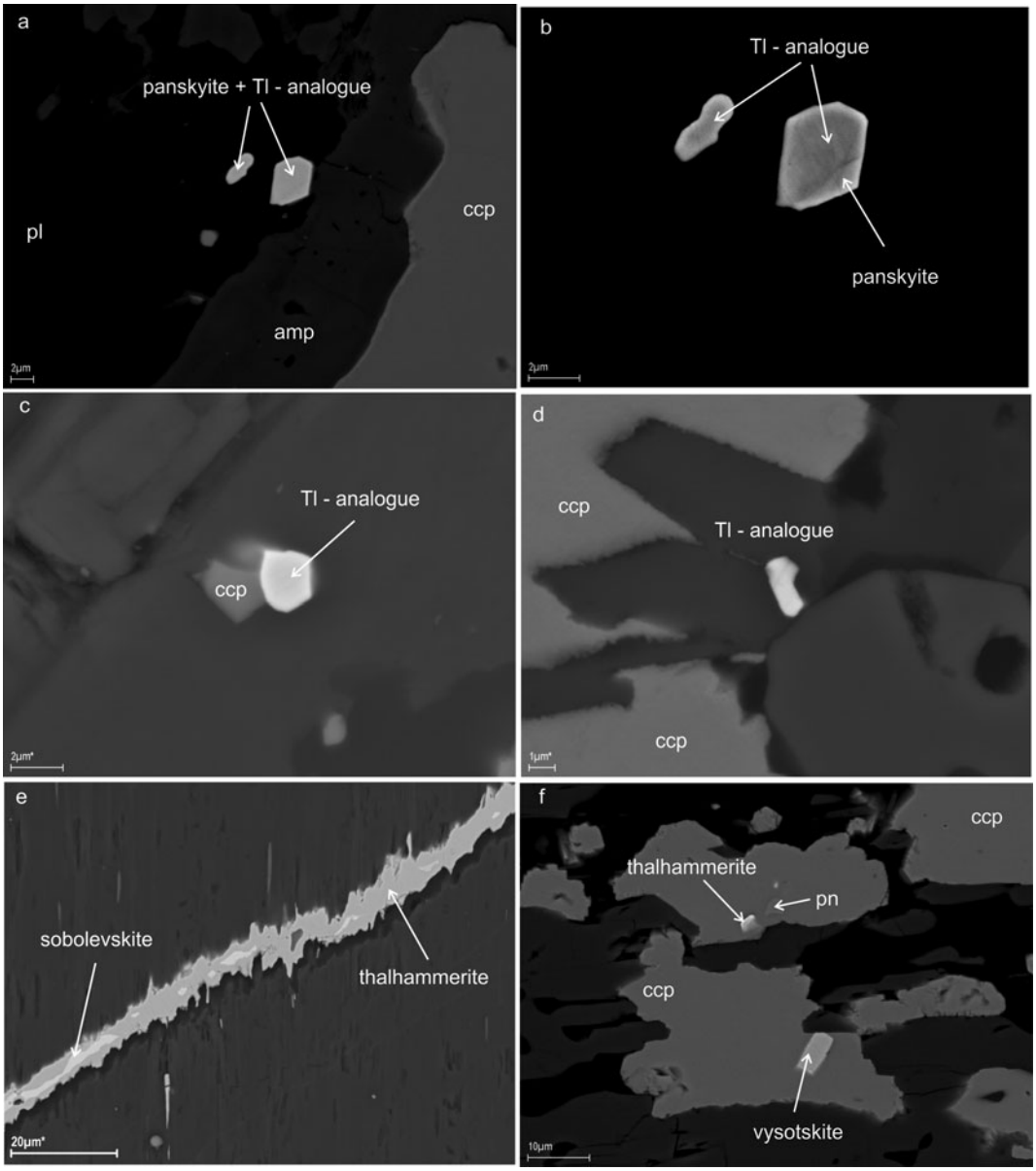

Fig. 3. Back-scattered electron images of panskyite, thalhammerite and its thallium analogue (unnamed phase $Pd_9Ag_2(Tl,Pb)_2S_4$) from West-Pana intrusion: (a) panskyite in an intergrowth with unnamed phase $Pd_9Ag_2(Tl,Pb)_2S_4$; (b) a detail; (c,d) unnamed phase $Pd_9Ag_2(Tl,Pb)_2S_4$; (e,f) thalhammerite. ccp – chalcopyrite, pn – pentlandite, pl – plagioclase and amp – amphibole. Samples are from: (a–d, f) Southern Kievey, (e) Northern Kamennik. For the location see Fig. 1; chemical composition is plotted on Fig. 4.

Synthetic analogue

The size (0.5–10 µm) of inclusions of panskyite, embedded in chalcopyrite or intergrown with other PGM, prevented its extraction in an amount required for relevant crystallographic and structural investigations. Therefore, these investigations were performed on its synthetic analogue.

Synthetic $Pd_9Ag_2Pb_2S_4$ phase was prepared using an evacuated silica glass tube method in the Laboratory of Experimental Mineralogy of the Czech Geological Survey in Prague. Palladium (99.95%), silver (99.999%), lead (99.9999%) and sulfur (99.999%) were used as starting materials for synthesis. The evacuated tube with its charge was sealed and annealed. After cooling by cold-water bath, the charge was ground into powder in acetone using an agate mortar, and thoroughly mixed to homogenise. The pulverised charge was sealed in an evacuated silica-glass tube again, and heated at 400°C for 7 months. The experimental product was quenched rapidly in cold water.

Chemical composition

Electron probe micro-analyses (EPMA) were performed with a CAMECA SX-100 electron probe microanalyser in wavelength-dispersive mode using an electron beam focussed to 1–2 µm. The standards used were pure elements for Pd, Ag and Ni; and

https://doi.org/10.1180/mgm.2020.100 Published online by Cambridge University Press

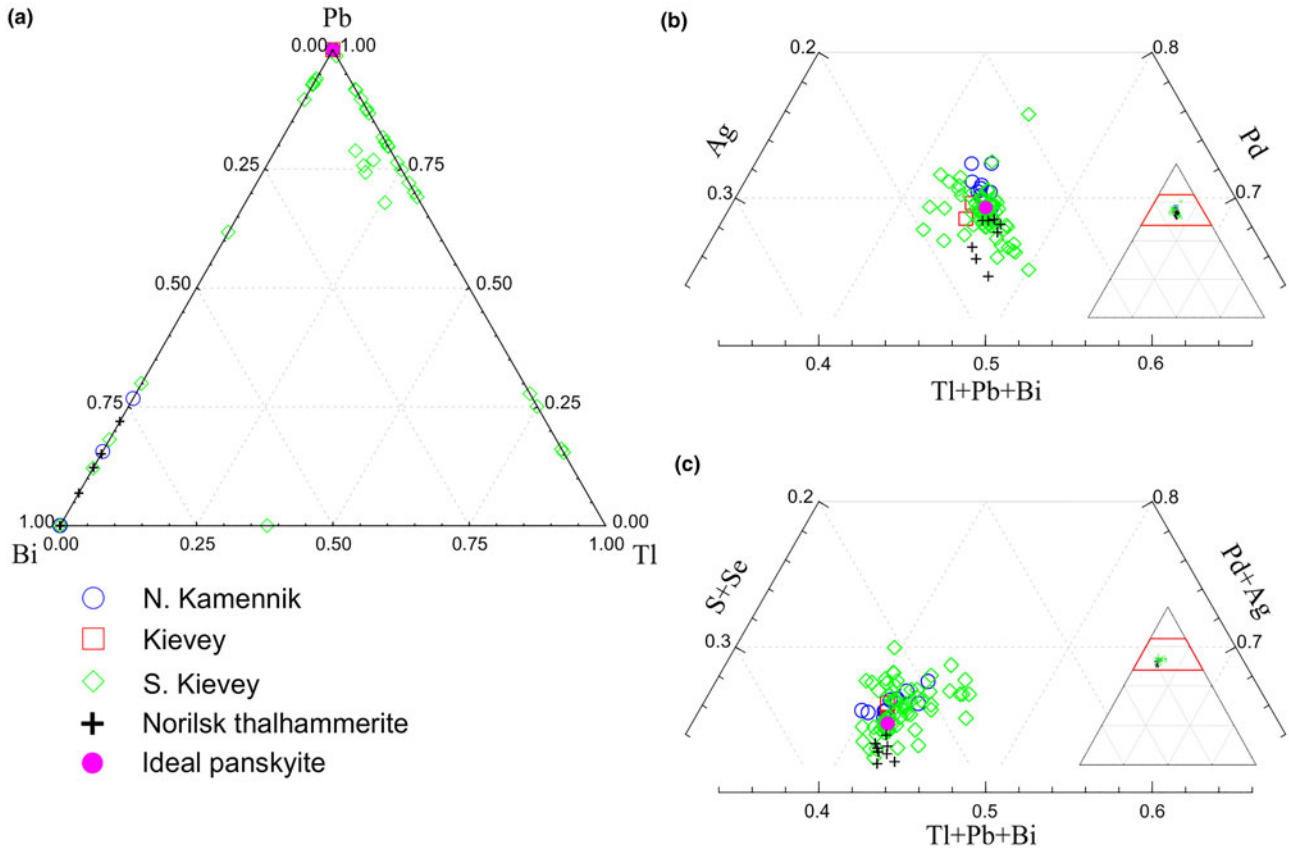

Fig. 4. Plot of compositional data for panskyite, thalhammerite and their thallium analogue (unnamed phase $Pd_9Ag_2(Tl,Pb)_2S_4$) from Northern Kamennik, Kievey and Southern Kievey, compared with thalhammerite from Noril`sk (Vymazalová *et al.*, 2018). The location of the samples studied is shown in Fig. 1.

galena for Pb and S. Concentrations were quantified on the Pd*L*α, Ag*L*α, Pb*M*α and S*K*α, with an accelerating voltage of 15 keV, and a beam current of 10 nA on the Faraday cup. Other elements were below the detection limit.

The EPMA results are given in Table 2. The EPMA data of natural material were collected on five different grains. The empirical formula, calculated for the mean composition ($n = 12$) on the basis of a total of 17 atoms per formula unit is $(Pd_{9.05}Fe_{0.07}Ni_{0.07})_{\Sigma 9.19}Ag_{1.98}Pb_{1.96}S_{3.87}$ for panskyite and $Pd_{9.07}Ag_{2.22}Pb_{1.78}S_{3.93}$ for its synthetic analogue, with an ideal formula $Pd_9Ag_2Pb_2S_4$.

Panskyite has a Bi analogue: thalhammerite; in addition we have observed its Tl-rich analogue from South Kievey. The compositional data of panskyite, thalhammerite and Tl analogues from North Kamennik, Kievey and South Kievey, compared with thalhammerite from Noril`sk are plotted in Fig. 4 (in total 88 analyses from SEM EDS and EPMA).

X-ray crystallography

Single-crystal X-ray diffraction

A small fragment of synthetic $Pd_9Ag_2Pb_2S_4$ was mounted on a glass fibre and examined using a Rigaku Super Nova single-crystal diffractometer with an Atlas S2 CCD detector utilising Mo*K*α radiation, provided by the microfocus X-ray tube and monochromatised by primary mirror optics. The ω rotational scans were used for the collection of three-dimensional intensity data. From 639 reflections, 186 were classified as unique observed with $I > 3\rho(I)$. Corrections for background, Lorentz effects and polarisation were applied during data reduction with *CrysAlis* software. Empirical absorption correction was performed using the same software yielding $R_{int} = 0.0308$. The crystal structure was solved with a charge-flipping method using the program *Superflip* (Palatinus and Chapuis, 2007) and subsequently refined by the full-matrix least-squares algorithm of *JANA2006* (Petříček *et al.*, 2014). Because of the similarity of the atomic number of Pd and Ag (46 and 47, respectively), it is nearly impossible to directly distinguish between these atoms from single-crystal (Mo*K*α radiation) diffraction data. The refinement indicated five metallic positions, of which one was assigned as Pb and the remaining four as Pd. The Pd sites show multiplicities 2:8:8:4. Considering the empirical chemical composition $Pd_{9.07}Ag_{2.22}Pb_{1.78}S_{3.93}$ ($Z = 2$) and coordination environment of the 4*e* site, which was very different from the others (see structure description), the 4*e* site was refined as the Ag position. An analogous situation was observed during the refinement of isostructural thalhammerite, $Pd_9Ag_2Bi_2S_4$ (Vymazalová *et al.*, 2018).

In subsequent refinement cycles, occupancy of all metallic sites was left free to vary (Pd *vs.* vacancy, Ag *vs.* vacancy and Pb *vs.* vacancy). While Pd and Ag sites were found to be fully occupied, refinement of the Pb position indicated 0.957(6) occupancy. Final anisotropic refinement in *I*4/*mmm* space group for 21 parameters converged smoothly to an $R_1 = 0.0227$ and $wR = 0.0260$ for 186

https://doi.org/10.1180/mgm.2020.100 Published online by Cambridge University Press

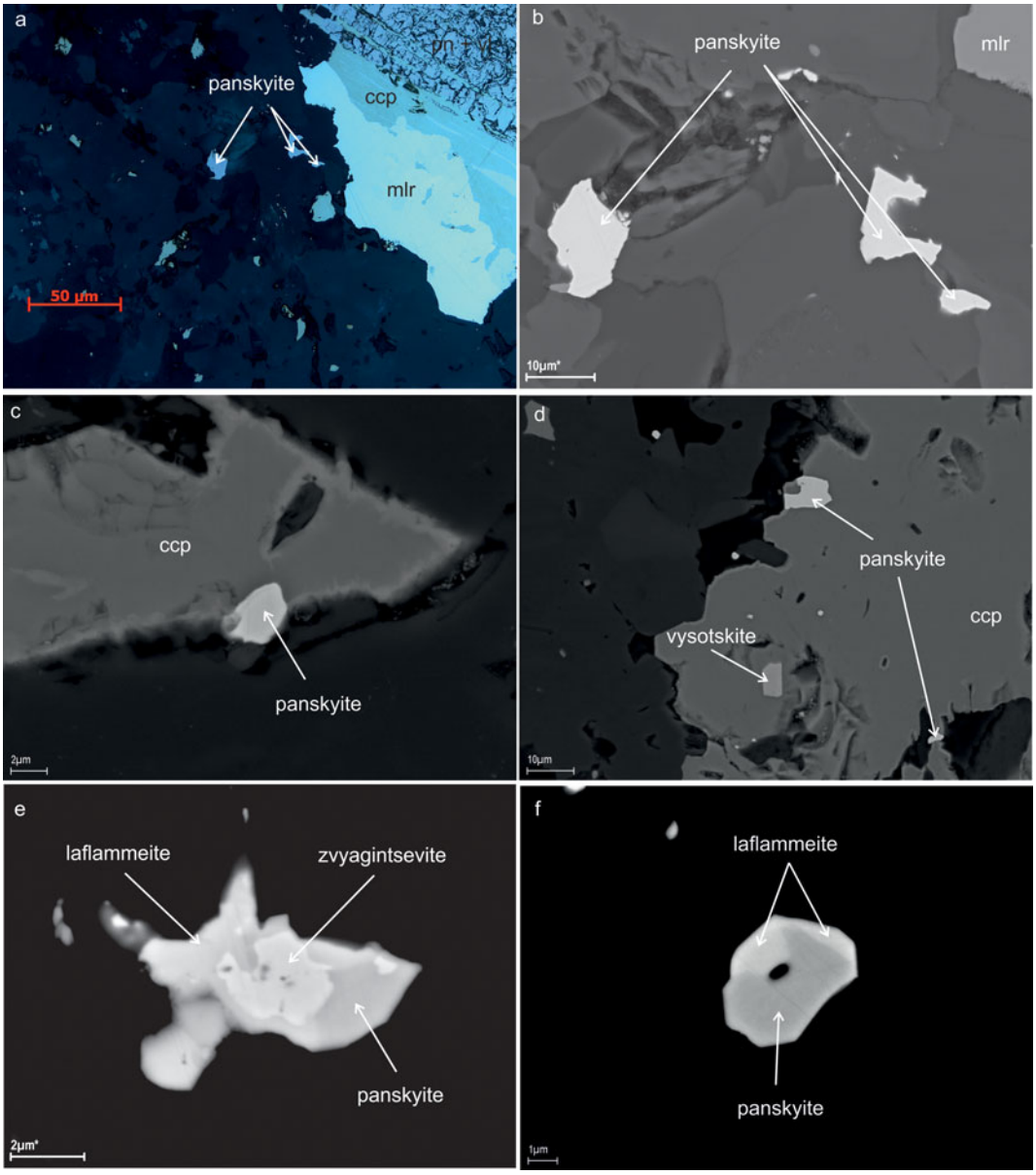

Fig. 5. Microphotographs of panskyite from the West-Pana intrusion: (a–d) in association with base-metal sulfides; (e,f) in intergrowths with other PGM (laflammeite and zvyagintsevite). (a) Reflected light, (b–f) back-scattered electron images. ccp – chalcopyrite, mlr – millerite, pn – pentlandite and vl – violarite. Samples are from Southern Kievey apart from (d) which is from Kievey; for sample locations see Fig. 1.

observed reflections. Details of data collection, crystallographic data and refinement are given in Table 3. Atom coordinates and displacement parameters are listed in Table 4. Table 5 shows selected bond lengths.

Powder X-ray diffraction

The powder X-ray diffraction pattern of synthetic panskyite was collected in Bragg–Brentano geometry on a Bruker D8 Advance diffractometer equipped with the LynxEye XE detector and Cu*K*α radiation. Data were collected in the range from 10° to 145°2θ with a step size of 0.005°2θ and 2 second counting time per step. The structure model obtained from a single-crystal X-ray study of panskyite was used in the subsequent Rietveld refinement. The program *Topas 5* (Bruker AXS, 2014) was used. The refinement involved refinement of scale factors, unit-cell parameters, isotropic size and strain. The background was determined by means of a Chebyshev polynomial function of the 5th order. No fractional coordinates were refined. The final cycles of refinement converged to the agreement factors $R_p = 7.92\%$ and $R_{wp} = 10.33\%$, the refinement indicated 0.5, 4 and 10 wt.% impurities of (Ag,Pb) alloy, PdS and Pd_3Pb, respectively. Powder X-ray diffraction data of the synthetic analogue of panskyite are summarised in Table 6. Fig. 7 shows the final Rietveld plot. The crystallographic information file has been deposited with the Principal Editor of *Mineralogical Magazine* and is available as Supplementary material (see below).

Table 1. Reflectance data for panskyite and its synthetic analogue, $Pd_9Ag_2Pb_2S_4$.

λ (nm)	Natural R_1	Natural R_2	Synthetic R_1	Synthetic R_2
400	41.5	41.8	41.4	41.9
420	42.2	42.6	41.8	42.5
440	42.9	43.2	42.4	43.1
460	43.6	43.8	43.1	43.5
470	**43.8**	**44.1**	**43.3**	**43.7**
480	43.9	44.3	43.5	43.8
500	44.1	44.5	43.7	43.9
520	44.1	44.5	44.0	44.1
540	44.3	44.6	44.4	44.6
546	**44.4**	**44.7**	**44.6**	**44.8**
560	44.7	45.0	45.0	45.3
580	45.3	45.5	45.7	46.0
589	**45.6**	**45.8**	**46.0**	**46.4**
600	45.9	46.0	46.3	46.8
620	46.4	46.5	46.9	47.6
640	47.0	46.9	47.5	48.4
650	**47.2**	**47.2**	**47.9**	**48.8**
660	47.4	47.4	48.2	49.3
680	48.2	47.9	48.9	50.3
700	49.1	48.4	49.5	51.3

The values required by the Commission on Ore Mineralogy are given in bold.

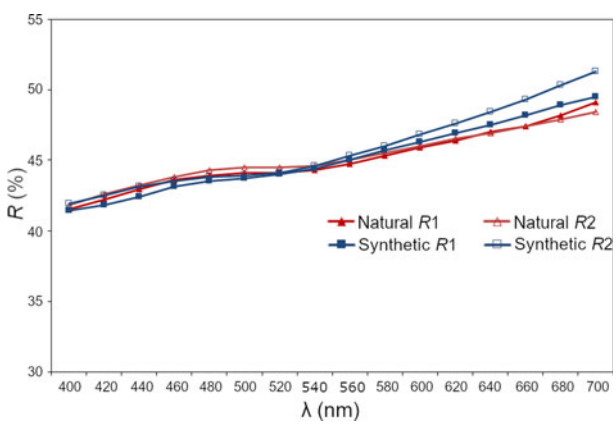

Fig. 6. Reflectance data for panskyite compared to its synthetic analogue, $Pd_9Ag_2Pb_2S_4$. The reflectance values (*R*, %) are plotted versus wavelength (λ, nm).

Table 2. EMPA data for panskyite and its synthetic analogue $Pd_9Ag_2Pb_2S_4$.

wt.%	Pd	Ag	Pb	S	Ni	Fe	Total
Panskyite							
grain 3-2a	56.28	11.95	23.48	7.41	0.24	0.21	99.36
grain 34b	55.28	12.19	23.45	7.21			98.12
grain 34b	55.70	12.19	23.37	7.13			98.38
grain 34b	54.75	12.37	23.72	7.23			98.06
grain 34b	55.78	12.45	24.01	7.15			99.39
grain 30d	55.54	12.79	23.48	7.07			98.88
Grain 30_7	55.27	12.41	23.13	6.90			97.71
grain 3-2a	55.00	12.27	23.44	7.19			97.91
grain 3-2b	56.28	12.31	23.67	7.25			99.51
grain 3-2b	56.05	12.63	23.44	7.20			99.31
grain 3-2b	55.90	12.31	23.76	7.01			98.98
grain 3-2a	55.47	12.49	23.03	7.28			98.27
Average	*55.61*	*12.36*	*23.50*	*7.17*	*0.24*	*0.21*	*98.66*
Synthetic analogue							
Average	57.02	14.17	21.81	7.44			100.44
Min	56.26	13.78	20.80	7.32			
Max	57.60	14.57	22.44	7.58			

Table 3. Crystallographic data for the selected crystal of the synthetic analogue of panskyite, $Pd_9Ag_2Pb_2S_4$.

Crystal data	
Chemical formula (idealised)	$Pd_9Ag_2Pb_2S_4$
Chemical formulae (from refinement)	$Pd_{9.00}Ag_{2.00}Pb_{1.91}S_{4.00}$
Space group	*I*4/*mmm* (No. 139)
a (Å)	7.973(3)
c (Å)	9.139(3)
V (Å^3)	581.0(4)
Z	2
Crystal size (mm)	0.054 × 0.017 × 0.010
Data collection	
Diffractometer	SuperNova
Temperature (K)	293
Radiation	Mo*K*α (0.7107 Å)
Theta range (°)	3.39–27.84
Reflections collected	639
Independent reflections	209
Unique observed reflections [*I*>3(σ)]	186
R_{int}	0.0308
Index ranges	$-7 < h < 8$
	$-10 < k < 7$
	$-11 < l < 7$
Absorption correction method	Empirical
Structure refinement	
Refinement method	Full matrix least-squares on F^2
Parameters/restrains/constrains	21/0/0
R, w*R* (obs)	0.0227/0.0260
R, w*R* (all)	0.0287/0.0293
Largest diff. peak and hole (e^-/Å^3)	1.55/−1.77

Structure description

The crystal structure of panskyite contains three distinct palladium sites and one silver, lead and sulfur site. Its crystal structure is shown in Fig. 8, selected coordination polyhedra in Fig. 9.

In panskyite, the Pd1 position forms square–planar coordination of S atoms at a distance of 2.346(3) Å. This coordination is perfectly planar and resembles that observed in vysotskite, PdS (Brese *et al.*, 1985). In addition to four S contacts, Pd1 atoms have two long contacts with Ag atoms oriented perpendicular to the [$Pd1S_4$] plane at a distance of 2.917(3) Å. The Pd2 site shows two short S and two Pb contacts at 2.329(4) and 2.7888(11) Å, respectively. Sulfur and Pb atoms make up a disphenoid, where Pd2 is placed in the middle of an S–S edge. This coordination is further completed by two Ag atoms at a distance of 2.904(2) Å. Consequently, the complete coordination sphere of Pd2 atoms can be described as an elongated tetragonal bipyramid [$Pd2S_2Pb_2Ag_2$] with the Ag atoms placed at a *cis* position (i.e. where Ag atoms are mutually adjacent). The central atom Pd2 is shifted slightly from the centre of the bipyramid towards the Pb–Pb edge. The coordination of Pd3 is similar to that of Pd2. Pd3 is surrounded by two S and Pb atoms forming a [$Pd3S_2Pb_2$] square and two additional Ag atoms at a distance of 2.8891(15) Å. The Ag atoms are oriented in a *trans* position (i.e. perpendicular to the [S_2Pb_2] square). Thus, the complete coordination sphere of the Pd3 site can be viewed as a compressed tetragonal bipyramid [$Pd3S_2Pb_2Ag_2$].

https://doi.org/10.1180/mgm.2020.100 Published online by Cambridge University Press

Table 4. Fractional coordinates and anisotropic displacement parameters (Å^2) for the synthetic analogue of panskyite, $Pd_9Ag_2Pb_2S_4$.

Atom	Wyckoff position	*x*	*y*	*z*	U^{11}	U^{22}	U^{33}	U^{12}	U^{13}	U^{23}	U_{eq}
Pd1	2*a*	0	0	0	0.0065(9)	0.0065(9)	0.0068(14)	0	0	0	0.0066(6)
Pd2	8*j*	0.20057(18)	½	0	0.0114(8)	0.0080(8)	0.0082(7)	0	0	0	0.0092(4)
Pd3	8*f*	¼	¼	¼	0.0125(6)	0.0125(6)	0.0070(8)	0.0008(6)	−0.0009(4)	−0.0009(4)	0.0107(4)
Ag	4*e*	0	0	0.3192(2)	0.0119(7)	0.0119(7)	0.0109(10)	0	0	0	0.0116(5)
Pb*	4*d*	0	½	¼	0.0099(5)	0.0099(5)	0.0099(6)	0	0	0	0.0099(3)
S	8*h*	0.2080(4)	0.2080(4)	0	0.0078(13)	0.0078(13)	0.008(2)	−0.0027(17)	0	0	0.0079(10)

*Refined with 0.96(1) occupancy.

Table 5. Selected bond distances (Å) in the synthetic analogue of panskyite, $Pd_9Ag_2Pb_2S_4$.

Pd1–S	2.346(3) ×4	Ag–Pd3	2.8891(15) ×4
Pd1–Ag	2.917(3) ×2	Ag–Pd2	2.904(2) ×4
		Ag–Pd1	2.917(2) ×1
Pd2–S	2.329(4) ×2		
Pd2–Pb	2.7888(11) ×2	Pb–Pd2	2.7888(16) ×4
Pd2–Ag	2.904(2) ×2	Pb–Pd3	2.8191(15) ×4
Pd2–Pd3	3.0574(8) ×4		
Pd3–S	2.3333(16) ×2		
Pd3–Pb	2.8191(15) ×2		
Pd3–Ag	2.8891(15) ×2		
Pd3–Pd2	3.0574(8) ×4		

Table 6. Powder X-ray diffraction data of synthetic analogue of panskyite (Cu*K*α radiation, Bruker D8 Advance, Bragg-Brentano geometry, 0.36° fixed divergence slit). Only reflections with $I_{(obs)} \geq 1$ are listed.

$I_{(obs)}$	$I_{(calc)}$	$d_{(obs)}$	$d_{(calc)}$	*h k l*
5	7	6.0202	6.0197	1 0 1
5	9	5.6527	5.6516	1 1 0
9	7	4.5757	4.5753	0 0 2
8	5	3.9973	3.9963	2 0 0
9	11	3.5564	3.5561	1 1 2
21	20	3.3298	3.3294	2 1 1
10	5	2.8499	2.8497	1 0 3
50	**49**	**2.8260**	**2.8258**	**2 2 0**
23	21	2.5581	2.5580	3 0 1
100	**100**	**2.4044**	**2.4042**	**2 2 2**
72	**60**	**2.3203**	**2.3202**	**2 1 3**
44	**37**	**2.2877**	**2.2876**	**0 0 4**
24	23	2.2125	2.2124	3 1 2
12	10	2.1206	2.1205	1 1 4
67	**52**	**1.9984**	**1.9982**	**4 0 0**
5	2	1.8838	1.8839	3 3 0
13	11	1.7931	1.7932	3 2 3
13	13	1.7781	1.7780	2 2 4
19	17	1.7420	1.7420	3 3 2
3	3	1.6361	1.6361	4 1 3
6	5	1.5083	1.5085	3 0 5
28	**28**	**1.5049**	**1.5049**	**4 0 4**
7	5	1.4724	1.4724	1 1 6
16	13	1.4128	1.4129	4 4 0
5	6	1.3500	1.3500	4 4 2
10	8	1.3421	1.3421	2 2 6
8	8	1.3345	1.3346	5 2 3
13	12	1.3058	1.3058	3 1 6
9	10	1.2638	1.2637	6 2 0
25	18	1.2179	1.2181	6 2 2
8	10	1.2021	1.2021	4 4 4
8	9	1.1853	1.1854	3 3 6
3	3	1.1438	1.1438	0 0 8
7	7	1.1061	1.1062	2 6 4

The strongest lines are given in bold.

Silver atoms are coordinated by nine Pd atoms at distances forming a monocapped tetragonal antiprism. The Ag–Pd distances are within the range from 2.8891(15) to 2.917(2) Å, which is comparable to those observed in kravtsovite, $PdAg_2S$ (Vymazalová *et al.*, 2017) and lukkulaisvaaraite $Pd_{14}Ag_2Te_9$ (Vymazalová *et al.*, 2014). The Ag atoms show weak Ag–Ag bonds at 3.304(4) Å across the shared tetragonal face (Fig. 9) of the antiprism. A lead atom has eight Pd contacts arranged in the form of bi-capped trigonal prism and showing a 4 + 4 bonding scheme. Observed Pd–Pb distances 2.7888(16) and 2.8191(15) Å are slightly shorter than corresponding Pd–Bi distances [2.808(1) and 2.8378(1) Å] observed in isostructural thalhammerite $Pd_9Ag_2Bi_2S_4$ (Vymazalová *et al.*, 2018). By analogy with thalhammerite, no short (<3.5 Å) Pb–S and Pb–Ag contacts occur in the panskyite crystal structure.

In terms of anion-centred polyhedra (Fig. 10), the S site has deformed trigonal–bipyramidal coordination with two Pd2, one Pd1 sites in equatorial and Pd3 in axial positions. While all Pd–S bonds are approximately equal (2.32–2.34 Å), the S atom is shifted from the polyhedra centre towards the Pd1 position thereby, reducing the Pd2–Pd2 distance in the equatorial plane to 3.37 Å and extending the Pd2–Pd1 distance to 4.29 Å. Consequently, the Pd2–Pd2–Pd1 atoms form an isosceles triangle instead of an equilateral one as in the case of regular coordination. The bipyramids share only corners (i.e. Pd atoms), forming a three-dimensional framework. While Pd3 and Pd2 vertices are shared with two adjacent bipyramids, four bipyramids are linked by sharing Pd3 vertices, producing four-fold 'iron crosses'. Lead and Ag atoms are placed in the voids in the framework forming Pb–Pd, Pd–Ag and Ag–Ag bonds. No short S–S bonds were observed. The shortest S–S distance of 3.316(5) Å is forced by the coordination geometry of adjacent cations.

Relation to other minerals

Panskyite is the Pb analogue of thalhammerite $Pd_9Ag_2Bi_2S_4$ (Vymazalová *et al.*, 2018). The main structural difference between these two minerals is that panskyite shows slightly shorter Pd–Pb bonds (2.803 Å on average) than the corresponding Pd–Bi bonds (2.822 Å on average) observed in thalhammerite. This is also reflected by a slightly smaller unit-cell volume of panskyite (581.0 Å^3) in comparison with thalhammerite (589.7 Å^3). Based on the chemical composition, there is also a Tl analogue (Fig. 3, 4); however, its crystal structure has not yet been studied.

Proof of identity of panskyite and its synthetic analogue

A TESCAN Mira 3GMU scanning electron microscope combined with an electron back-scatter diffraction (EBSD) system

https://doi.org/10.1180/mgm.2020.100 Published online by Cambridge University Press

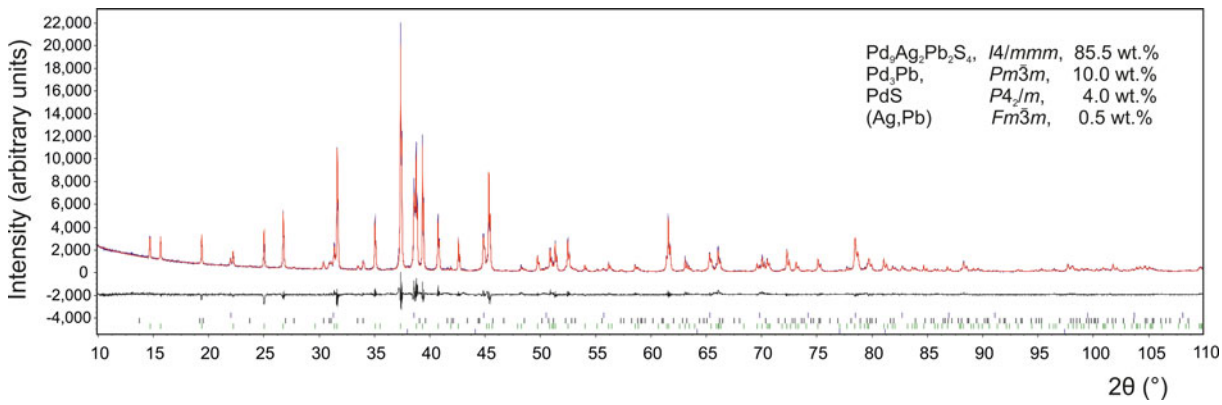

Fig. 7. The final Rietveld fit of the synthetic analogue of panskyite, $Pd_9Ag_2Pb_2S_4$. The sample contains ca. 10, 4.0 and 0.5 wt.% Pd_3Pb, PdS and (Ag,Pb) alloy as impurities, respectively.

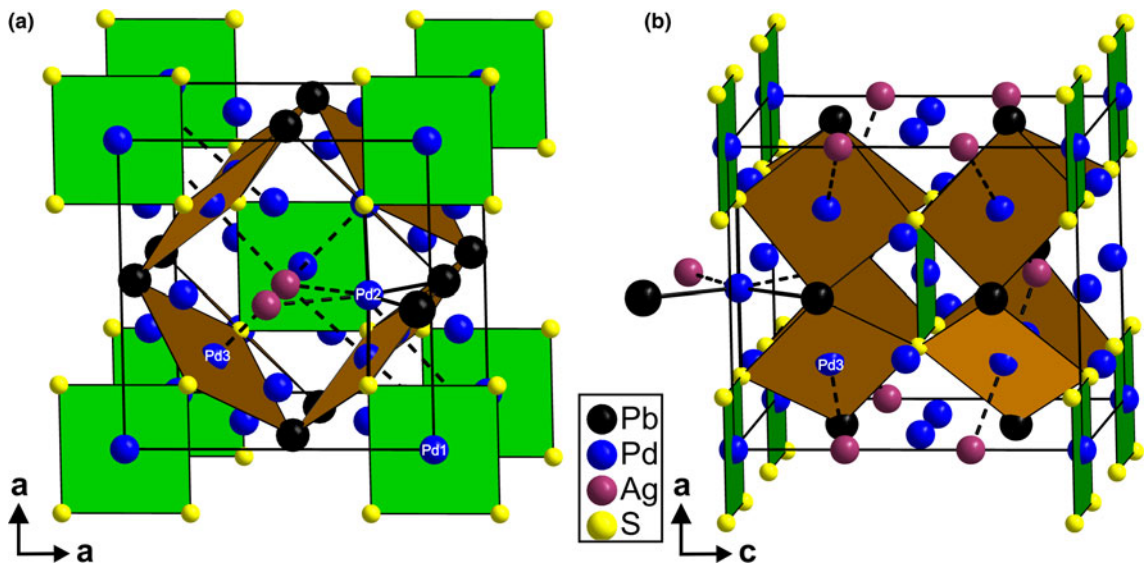

Fig. 8. Crystal structure of the synthetic analogue of panskyite showing [Pd1S_4] (green) an [Pd3Pb_2S_2] (orange) squares. (a) View along **c** and (b) view along **a** axis. Ag–Pd interactions are indicated by dashed lines, coordination environment of one Pd2 is shown in (a).

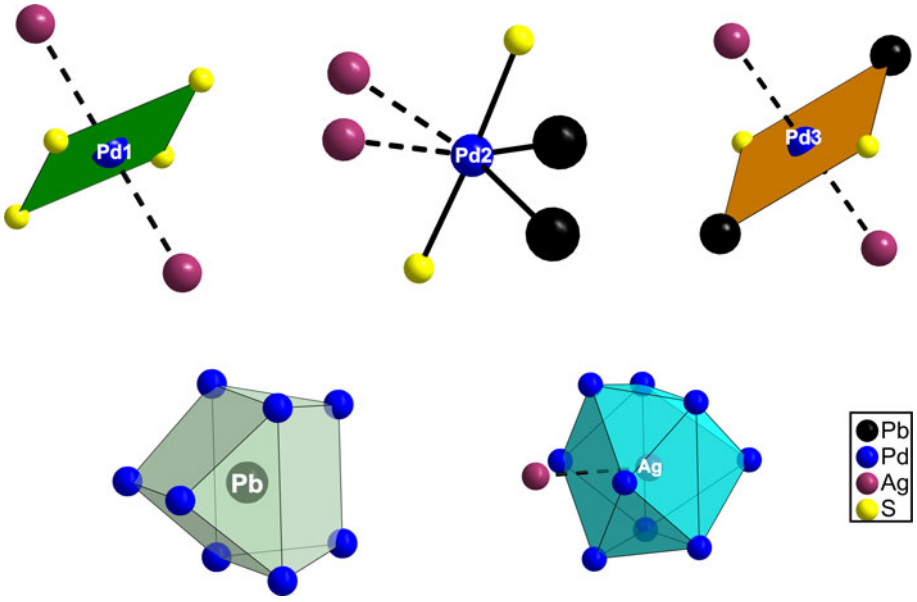

Fig. 9. Coordination polyhedra of Pd1, Pd2, Pd3, Pb and Ag sites in the panskyite crystal structure. Weak Ag–Pd and Ag–Ag interactions are indicated by dashed lines.

https://doi.org/10.1180/mgm.2020.100 Published online by Cambridge University Press

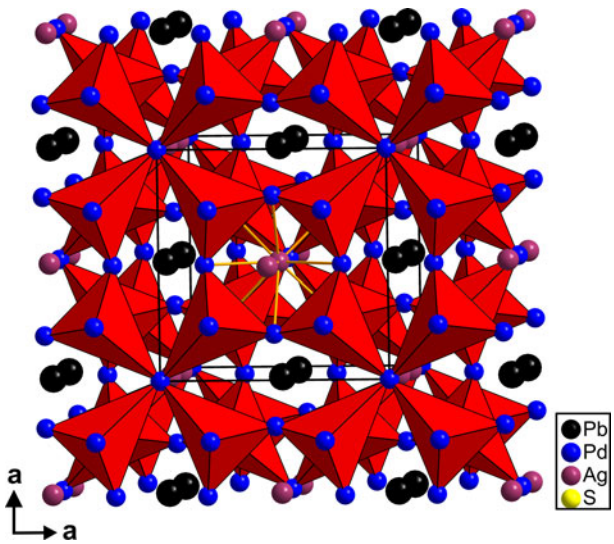

Fig. 10. Crystal structure of panskyite showing a corner-sharing anion-based trigonal-bipyramids [SPd]. Ag–Ag and Ag–Pd interactions are indicated in the middle of the Figure. Note the four-fold 'iron crosses' of [SPd_5] coordination bipyramids.

(Nordlys Nano detector, Oxford Instruments) was used for the measurements. The sample surface was prepared for EBSD by polishing with colloidal silica (OP-U) for 30 min. Acquisition conditions were: accelerating voltage 20 kV, beam current ~3 nA, no binning (full EBSP resolution is 1344 × 1024). Indexing conditions were: refined accuracy mode, 8 bands, 44 reflectors. The EBSD patterns were collected and processed using a proprietary computer program: *AZtec HKL* (Oxford Instruments). The solid angles calculated from the patterns were compared with a structural model proposed match containing 44 reflectors to index the patterns. EBSD patterns (also known as Kikuchi patterns) obtained from the natural material (20 measurements on different grains of panskyite) were found to match the patterns generated from our refined structural model for $Pd_9Ag_2Pb_2S_4$ (Fig. 11). The values of the mean angular deviation (MAD, i.e. the goodness of fit of the solution) between the calculated and measured Kikuchi bands range between 0.22° and 0.44°. These values reveal a very good match; as long as values of mean angular deviation are <1°, they are considered as indicators of an acceptable fit (HKL Technology v. 2004).

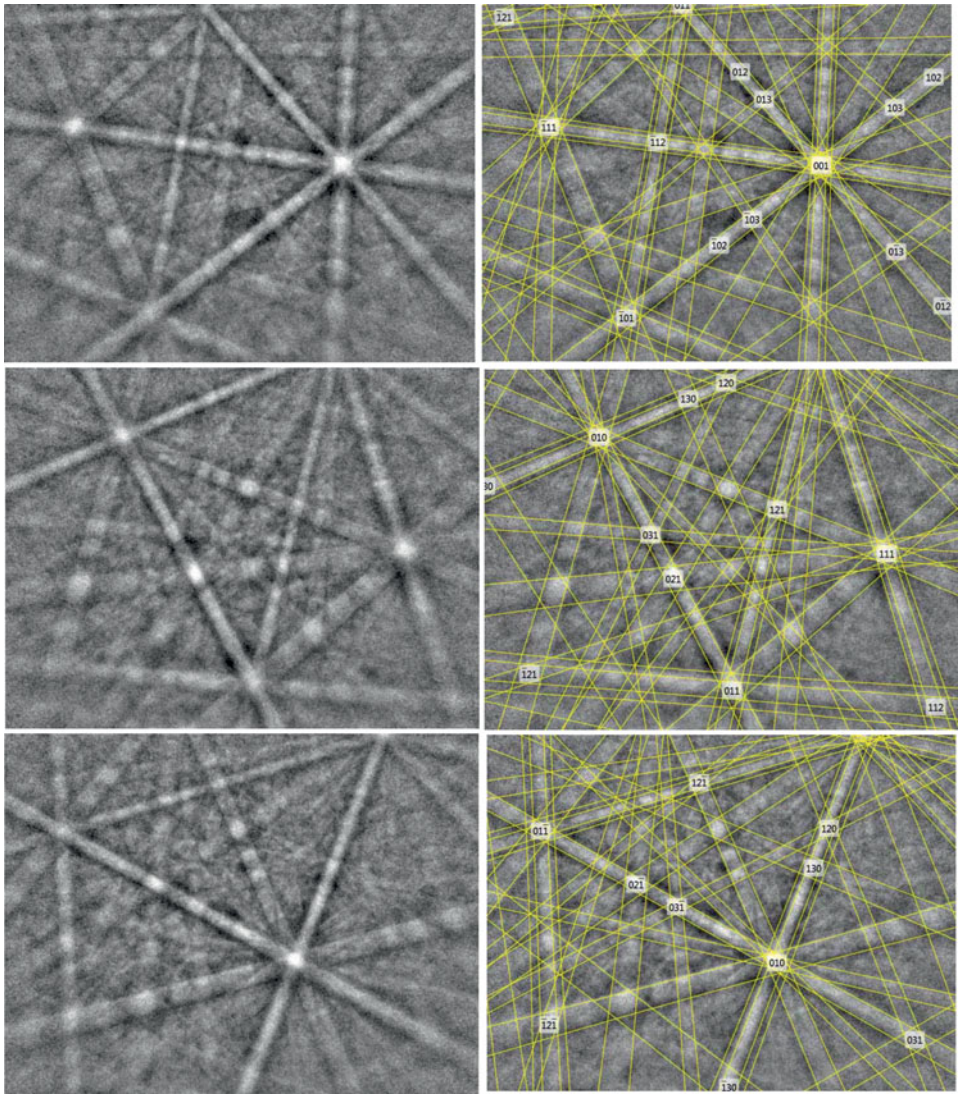

Fig. 11. Electron back-scattered diffraction patterns (EBSPs) showing different orientations of grains of panskyite; in the right pane, the Kikuchi bands are solved (indexed).

https://doi.org/10.1180/mgm.2020.100 Published online by Cambridge University Press

Acknowledgments. The authors acknowledge Ritsuro Miyawaki, Chairman of the IMA-CNMNC and its members, for helpful comments on the submitted data. The reviewer's comments of Louis J. Cabri, an anonymous reviewer, Structures Editor Peter Leverett and the Principle Editor Stuart Mills are greatly appreciated. This research was supported by the Grant Agency of the Czech Republic (project No. 18-15390S to A.V.), by the Czech Geological Survey (DKRVO/ČGS 2018–2022), and by the Operational Programme Research, Development and Education financed by European Structural and Investment Funds and the Czech Ministry of Education, Youth and Sports (Project No. SOLID21 CZ.02.1.01/0.0/0.0/16_019/0000760). C.J. Stanley acknowledges Natural Environment Research Council grant NE/M010848/1 Tellurium and selenium cycling and supply. We are also grateful to Dr. Alexey U. Korchagin, General Director of Pana JSC, for his assistance in conducting research and preparing the publication.

Supplementary material. To view supplementary material for this article, please visit https://doi.org/10.1180/mgm.2020.100

References

Brese N.E., Squattrito P.J. and Ibers J.A. (1985) Reinvestigation of the structure PdS. *Acta Crystallographica*, **C41**, 1829–1830.

Bruker AXS (2014) *Topas 5, Computing Program*. Bruker AXS GmbH, Karlsruhe, Germany.

Korchagin A.U. and Mitrofanov F.P. (2008) Deposits of PGE of the Western part of Fedorovo–Pana Tundra (Fedorovo and Malaya Pana): status and development prospects. Pp. 43–52 in: *An Interreg Tacis Project: Strategic Mineral Resources of Lapland – Base for the Sustainable Development of the North*. Project publication, volume I. KSC Russian Academy of Science, Apatity, Russia.

Korchagin A.U., Subbotin V.V., Mitrofanov F.P. and Mineev S.D. (2009) Kievey PGE-bearing deposit in the West Pana layered intrusion. Pp. 12–32 in: *An Interreg Tacis Project: Strategic Mineral Resources of Lapland – Base for the Sustainable Development of the North*. Project publication, volume II. KSC Russian Academy of Science, Apatity, Russia.

Korchagin A.U., Goncharov Yu.V., Subbotin V.V., Groshev N.Yu., Gabov D.A., Ivanov A.N. and Savchenko Ye.E. (2016) Geology and ores composition of the North Kamennik low-sulfide PGE deposit in the West–Pansky massif, Kola Peninsula. *Ore and Metals*, **1**, 42–51 [in Russian].

Naldrett A.J. (2004) *Magmatic Sulphide Deposits: Geology, Geochemistry and Exploration*. Springer Verlag, New York, 728 p.

Palatinus L. and Chapuis G. (2007) SUPERFLIP – a computer program for the solution of crystal structures by charge flipping in arbitrary dimensions. *Journal of Applied Crystallography*, **41**, 786–790.

Petříček V., Dušek M. and Palatinus, L. (2014) Crystallographic Computing System JANA2006: General features. *Zeitschrift für Kristallographie*, **229**, 345–352.

Schissel D., Tsvetkov A.A., Mitrofanov F.P. and Korchagin A.U. (2002) Basal platinum-group element mineralization in the Federov Pansky layered mafic intrusion, Kola Peninsula, Russia. *Economic Geology*, **97**, 1657–1677.

Smith D.G.W. and Nickel E.H. (2007) A system for codification for unnamed minerals: report of the Subcommittee for Unnamed Minerals of the IMA Commission on New Minerals, Nomenclature and Classification. *The Canadian Mineralogist*, **45**, 983–1055.

Subbotin V.V., Gabov D.A., Korchagin A.U. and Savchenko E.E. (2017) Gold and silver in the composition of PGE ores of the Fedorovo–Pana Layered Intrusive Complex. *Herald of the Kola Science Centre of the RAS*, **1**, 53–65 [in Russian].

Subbotin V.V., Vymazalová A., Laufek F., Savchenko Y.E., Stanley C.J. Gabov D.A and Plášil J. (2019) Mitrofanovite, Pt_3Te_4, a new mineral from the East Chuarvy deposit, Fedorovo–Pana intrusion, Kola Peninsula, Russia. *Mineralogical Magazine*, **83**, 523–530.

Vymazalová A., Grokhovskaya T.L., Laufek F. and Rassulov V.A. (2014) Lukkulaisvaaraite, $Pd_{14}Ag_2Te_9$, a new mineral from Lukkulaisvaara intrusion, northern Russian Karelia, Russia. *Mineralogical Magazine*, **78**, 1743–1754.

Vymazalová A., Laufek F., Sluzhenikin S.F., Stanley C.J., Kozlov V.V., Chareev D.A. and Lukashova M.L. (2017) Kravtsovite, $PdAg_2S$, a new mineral from Noril'sk – Talnakh deposit, Russia. *European Journal of Mineralogy*, **29**, 597–602.

Vymazalová A., Laufek F., Sluzhenikin S.F., Kozlov V.V., Stanley C.J., Plášil J., Zaccarini F., Garuti G. and Bakker R. (2018) Thalhammerite, $Pd_9Ag_2Bi_2S_4$, a new mineral from the Talnakh and Oktyabrsk deposits, Noril'sk region, Russia. *Minerals*, **8**, 339.

Vymazalová A., Subbotin V.V., Laufek F., Savchenko Y.E., Stanley C.J., Gabov D.A. and Plášil J. (2020) Panskyite, IMA 2020–039. CNMNC Newsletter No. 57; *Mineralogical Magazine*, **84**, https://doi.org/10.1180/mgm.2020.73